Phase Transformations in $Ag_{48}Zn_{50}Au_2$ and $Ag_{48}Zn_{50}Cu_2$ Alloys

M. GRANOVSKY, M. RESTA LEVI, AND D. ARIAS

Comisión Nacional de Energía Atómica, Avenida del Libertador 8250, 1429 Buenos Aires, Argentina

The order–disorder phase transformation temperatures for $Ag_{48}Zn_{50}Au_2$ and $Ag_{48}Zn_{50}Cu_2$ alloys have been determined using resistivity techniques and the ordering energies of the closest neighbors of the Au–Zn and Ag–Cu pairs calculated. Investigation of the kinetics of the $\beta' \rightarrow \zeta_0$ phase transformation using resistivity, metallographic, microanalytical, and x-ray techniques showed a two-phase field in both alloys, corresponding to the $\beta' + \zeta_0$ phases.

Introduction

In the region of equiatomic composition, the Ag–Zn system has a body-centered-cubic disordered β phase at temperatures above 274°C. On quenching from a higher temperature, it transforms to the ordered Cs–Cl structure. Slow cooling from above the same temperature and isothermal annealing in the range 100–274°C produce a complex hexagonal structure ζ_0 [1].

The order–disorder reaction $\beta' \leftrightarrows \beta$ and the $\beta' \rightarrow \zeta_0$ phase transformation have previously been studied in $Ag_{50}Zn_{50}$ [2–6] and in the ternary systems $Ag_{50-x}Zn_{50}Au_x$ ($x \geq 3$) [7, 8] and $Ag_{53-x}Zn_{47}Cu_x$ ($4 > x > 1$) [9]. In the second the ζ_0 phase has not been reported. In the third an increase in the ζ_0 transformation temperature with Cu content has been observed. These results show that Au and Cu determine an increase in the stability of the ordered phases, which may be related, respectively, to the electronegativity differences between Au–Zn and Ag–Zn pairs and to a dependence on atomic diameter.

In the present work 2% Ag atoms were replaced by Au or Cu in the $Ag_{50}Zn_{50}$ base alloy in order to obtain a ternary alloy with the same electron concentration ($e/a = 1.5$) and in which, notwithstanding the increase in stability of the ordered phase, the transformation $\beta' \rightarrow \zeta_0$ would be possible. The purpose of the present work was to measure the

0026-0800/82/030213 + 12$02.75

order–disorder temperature, to study the $\beta' \rightarrow \zeta_0$ phase transformation in $Ag_{48}Zn_{50}Cu_2$ and $Ag_{48}Zn_{50}Au_2$ alloys, and to analyze the crystallographic structures and composition of the different phases involved in both alloys.

Experimental Procedure

ALLOY PREPARATION

Special 99.999+% Ag, Zn, and Cu and special 99.9999% Au were melted to make the alloys. The alloying elements were melted in quartz tubes under a partial pressure of high purity argon. The alloys were mixed by shaking the tubes while the metal was molten. The assumed composition of the alloys was used whenever weight losses were less than 0.1%. In some cases microprobe and wet analysis were employed to confirm the alloy composition. The ingots were sealed in quartz tubes containing high purity argon and homogeneized for 240 hr at 600°C. After cooling they were cold rolled with an intermediate anneal at 400°C. Sheet samples 0.1 mm thick were then prepared.

RESISTIVITY EXPERIMENTS

The order–disorder temperature T_0 was studied using four-terminal resistivity techniques. Polycrystalline strips measuring $1 \times 0.1 \times 50$ mm were prepared. Current and voltage leads were made using the binary base $Ag_{50}Zn_{50}$ alloy, and 0.2 mm calibrated copper Constantan thermocuples wires were spot welded to the sheets. Voltage and external resistance settings were chosen to maintain a constant current through the specimen so that the output from the voltage taps was directly proportional to the resistivity. Temperature and voltage changes were recorded continuously using an X–Y recorder. A silicone oil bath was used for the heat treatments. The samples were heated or cooled between room temperature and 350°C using rates, between 30 C°/sec and 0.5 C°/min in order to measure T_0. Metallographic studies were made on every cooled sample to verify the $\beta \rightarrow \beta'$ reaction. In all cases samples showed the classical pink color of the β' phase.

The kinetics of the isothermal $\beta' \rightarrow \zeta_0$ phase transformation in $Ag_{48}Zn_{50}Cu_2$ was studied by measuring the changes in the electrical resistivity, assuming that the resistivity was proportional to the transformed fraction, as in $Ag_{50}Zn_{50}$ [4]. In order to retain the β' phase, the samples were quenched in carbon tetracloride at 0°C after 30 min heat treatment

at 350°C in the silicone oil bath. The isothermal heat treatments were made in the same bath between 170 and 230°C (± 1°C).

X-RAY TECHNIQUE AND ELECTRON MICROPROBE ANALYSIS

The samples were sealed in glass tubes back-filled with high-purity argon and quenched in double-distilled water, causing the tubes immediately to crack. The crystal structures were studied for the $Ag_{48}Zn_{50}Cu_2$ and $Ag_{48}Zn_{50}Au_2$ β′-phase powder alloys after 1 hr heat treatment at 375°C and a quench to room temperature. Powder Debye–Scherrer techniques were employed to obtain x-ray patterns using a 57.3-mm-diam camera and Cu radiation. $Ag_{50}Zn_{50}$ powder alloy also was heat treated, to allow comparison of the x-ray results. The $\beta' \rightarrow \zeta_0$ transformation was then analyzed using the same techniques after the following schedule:

1. heat treatment for 0.5 hr at 403°C (β phase);
2. quench to room temperature (β′ phase);
3. isothermal heat treatment to obtain the ζ_0 phase: ($Ag_{50}Z_{50}$ 1 hr at 197°C, $Ag_{48}Zn_{50}Cu_2$ 260 hr at 230°C, and $Ag_{48}Zn_{50}Au_2$ 2040 hr at 250°C); and
4. quench to room temperature $Ag_{50}Zn_{50}$ (ζ_0) or $Ag_{48}Zn_{50}Cu_2$ and $Ag_{48}Zn_{50}Au_2$ ($\zeta_0 + \beta'$).

The times and annealing temperatures were chosen taking into account the different kinetic behavior of the three alloys.

The homogeneity of composition was confirmed using a Cameca electron microprobe. The chemical quantitative analyses were performed with the same electron microprobe.

Results

ORDER–DISORDER TEMPERATURE

Figures 1 and 2 show heating and cooling resistivity–temperature curves for the $\beta' \rightleftarrows \beta$ reactions corresponding to the alloys $Ag_{48}Zn_{50}Cu_2$ and $Ag_{48}Zn_{50}Au_2$, respectively. The shape of each curve is similar to that for $Ag_{50}Zn_{50}$ [3, 6]. T_0 was assumed to be the temperature at which $d\rho/dT$ is a maximum, where $d\rho/dT$ is related to the derivatives with respect to temperature of the long- and short-range order parameters [3, 10]. The order–disorder temperatures were calculated by averaging data from

more than 40 tests. The results were $T_0 = 256 \pm 5°C$ for $Ag_{48}Zn_{50}Cu_2$ and $T_0 = 296 \pm 5°C$ for $Ag_{48}Zn_{50}Au_2$.

$\zeta_0 \rightarrow \beta$ PHASE TRANSFORMATION

From curve a in Fig. 1, corresponding to the transformation $\zeta_0 \rightarrow \beta$, a narrow two-phase field ($\zeta_0 + \beta$) between approximately 261 and 268°C is suggested for $Ag_{48}Zn_{50}Cu_2$. An analogous result for $Ag_{50}Zn_{50}$, but at a temperature 6°C higher, has been reported [3].

$\beta' \rightarrow \zeta_0$ PHASE TRANSFORMATION

The experimental results corresponding to the different isothermal treatments of $Ag_{48}Zn_{50}Cu_2$ samples were interpreted using the John-

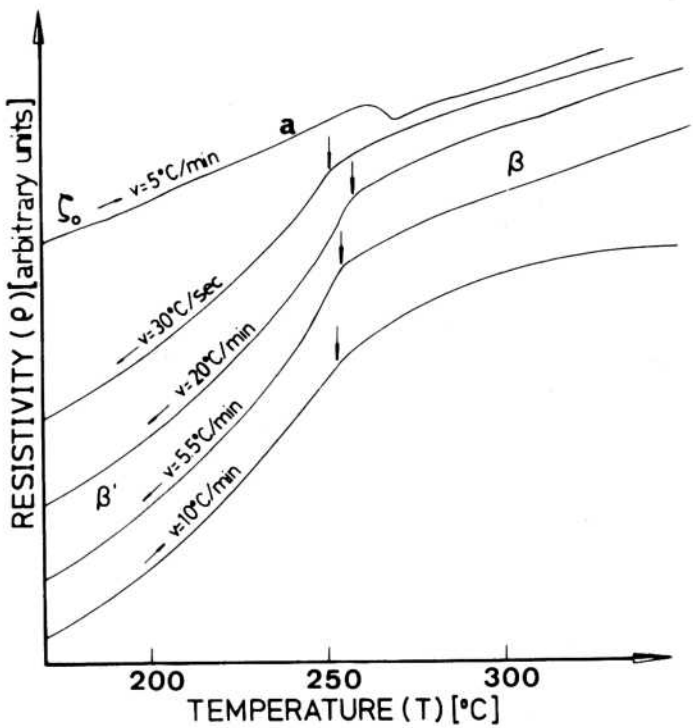

FIG. 1. $Ag_{48}Zn_{50}Cu_2$ resistivity vs temperature curves for different cooling or heating rates corresponding to the $\zeta_0 \rightarrow \beta$ phase transition and $\beta' \rightleftarrows \zeta_0$ reaction. Vertical arrows indicate the order–disorder temperature T_0 (such that $d\rho/dT$ is a maximum).

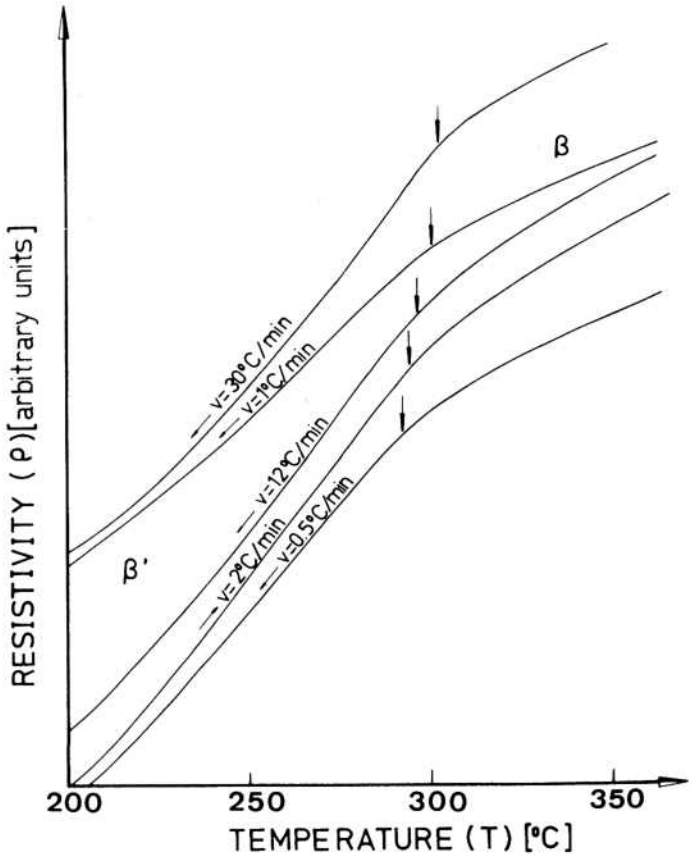

FIG. 2. $Ag_{48}Zn_{50}Au_2$ resistivity vs temperature curves for different cooling or heating rates corresponding to the $\beta' \rightleftarrows \beta$ reaction. Vertical arrows indicate the order–disorder temperature T_0.

son–Mehl–Avrami equation [11],

$$X = 1 - \exp(-k^n t^n),$$

were X is the transformed fraction, t is the transformation time, k is the reaction constant, and n is a constant associated with the details of a nucleation and growth process.

Figure 3 shows experimentally determined plots of $\ln \ln[1/(1 - X)]$ vs $\ln t$. In all kinetics two slopes corresponding to very different n values were observed. The first can be associated with a nucleation and growth process, the second with a diffusion process. These results suggest a two-phase field.

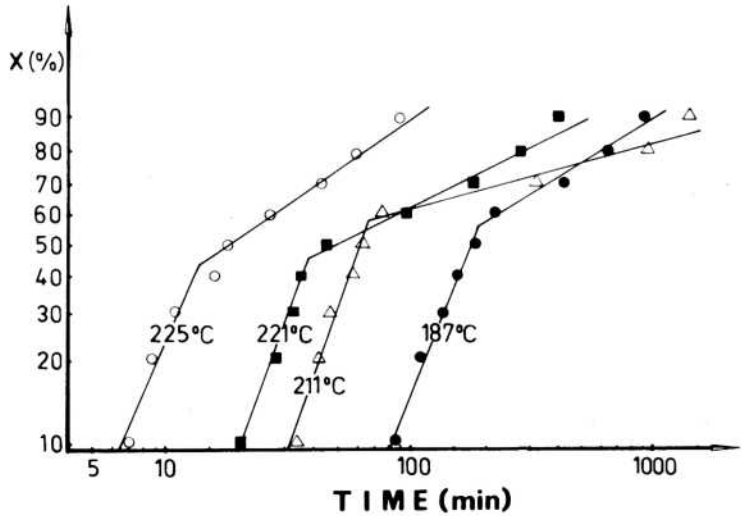

FIG. 3. $Ag_{48}Zn_{50}Cu_2$ kinetic decomposition results, plotted in terms of the Johnson–Mehl–Avrami equation, as $\ln \ln[1/(1 - X)]$ vs $\ln t$ (where X is the transformed fraction).

Owing to limitations in the experimental facilities, it was not possible to use resistivity techniques to study the $Ag_{48}Zn_{50}Au_2$ $\beta' \rightarrow \zeta_0$ phase transformation, but observations were made metallographically.

Figure 4(a, b) shows microstructures of $Ag_{48}Zn_{50}Cu_2$ heat treated at 230°C for two different time periods. In Fig. 4(a), taken after 10 hr exposure, the structure contains areas of β' and ζ_0; ζ_0, however, contains stringers of β'. After 25 hr [Fig. 4(b)] no single-phase β' was detected. Microstructures of the alloy $Ag_{48}Zn_{50}Au_2$ are shown in Figure 4(c, d) after 240 and 744 hr, respectively, at 275°C. The $\beta' \rightarrow \zeta_0$ transformed fraction shows a marked increase over this aging period. For comparative purposes, microstructural development in $Ag_{50}Zn_{50}$ is shown after 0.3 and 0.7 hr at 145°C [Fig. 4(e, f)].

The crystallographic structure of phases present in the three alloys were determined from x-ray diffraction patterns and indexed by means of the Hull–Davey chart [12]. An ordered cubic structure was found in the quenched samples (Table 1). After the heat treatment and quench schedule given here, the $Ag_{50}Zn_{50}$ and $Ag_{48}Zn_{50}Cu_2$ x-ray patterns showed, to within experimental error, the characteristic ζ_0 complex hexagonal phase lines while the $Ag_{48}Zn_{50}Au_2$ x-ray patterns showed the $\zeta_0 + \beta'$ ordered cubic phase line (Table 2). Since it was not possible by x-ray analysis to identify the structure corresponding to the $Ag_{48}Zn_{50}Cu_2$ β' "stringers," the homogeneity of composition was studied in the heat-treated samples.

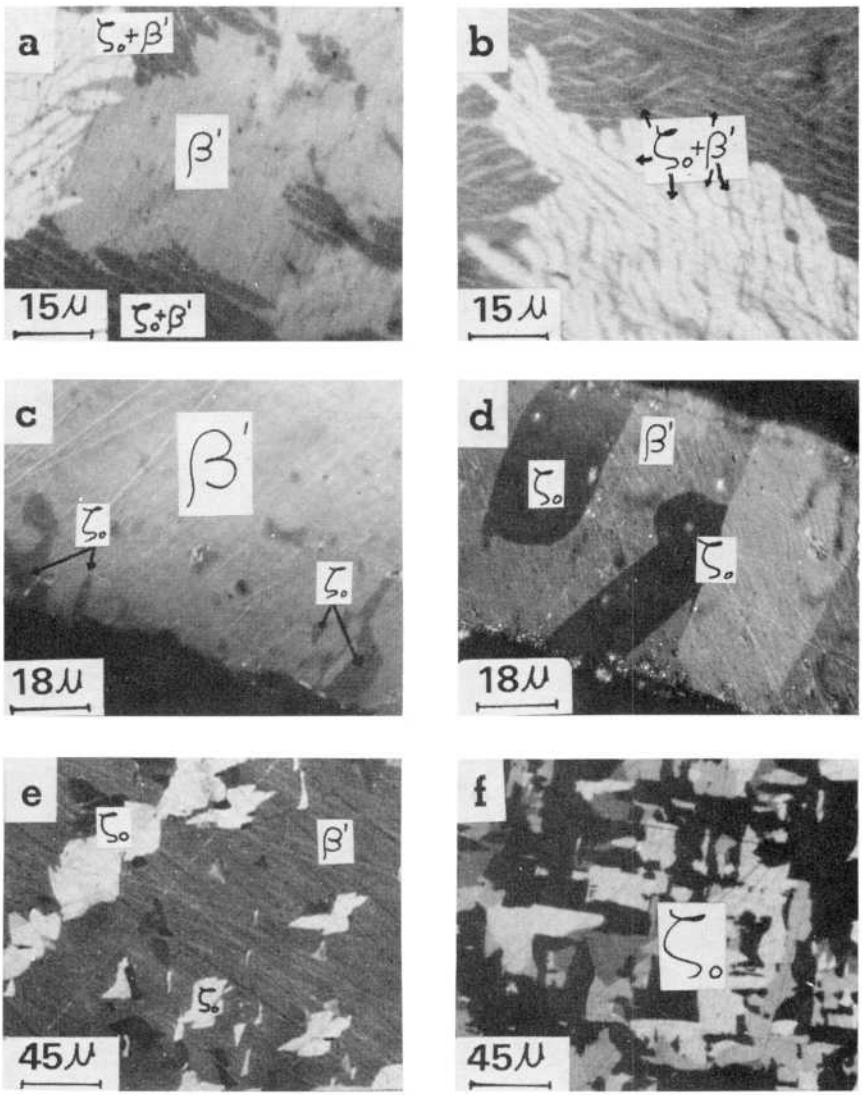

FIG. 4. Metallographies corresponding to (a) $Ag_{48}Zn_{50}Cu_2$ (230°C for 10 hr), (b) $Ag_{48}Zn_{50}Cu_2$ (230°C for 25 hr), (c) $Ag_{48}Zn_{50}Au_2$ (275°C for 240 hr), (d) $Ag_{48}Zn_{50}Au_2$ (275°C for 744 hr), (e) $Ag_{50}Zn_{50}$ (145°C for 0.3 hr), and (f) $Ag_{50}Zn_{50}$ (145°C for 0.7 hr).

TABLE 1
Interplanar Crystalline Distances (in angstroms) Corresponding to the β′ Ordered Cubic Phase for $Ag_{48}Zn_{50}Cu_2$, $Ag_{48}Zn_{50}Au_2$, and $Ag_{50}Zn_{50}$ Quenched to Room Temperature

hkl	$Ag_{48}Zn_{50}Cu_2$	$Ag_{48}Zn_{50}Au_2$	$Ag_{50}Zn_{50}$
100	3.12	3.10	3.13
110	2.21	2.20	2.23
111	1.80	1.80	1.82
200	1.57	1.56	1.57
210	1.40	1.40	1.41
211	1.28	1.28	1.28
220	1.11	1.11	1.11
221	1.05	1.05	1.05
310	0.99	0.99	1.00
311	0.95	0.95	—
222	0.91	0.91	0.91
320	0.87	0.87	0.87
321	0.84	0.84	0.84
400	0.79	0.79	—

Inhomogeneities in composition were observed in both alloys. Figure 5(a) shows the Cu-enriched zones in the $Ag_{48}Zn_{50}Cu_2$ alloy associated with the β′ phase, as indicated in the pseudo-ternary $CuAgZn_{47}$ phase diagram proposed by Yono et al. [9]. Figure 5(b) shows an Au-enriched zone in the $Ag_{48}Zn_{50}Au_2$ alloy, also associated with the β′ phase. This enrichment may be similar to the replacement of Ag by Au in AgZn, which increases the stability of the β′ with respect to the ζ_0 phase [7].

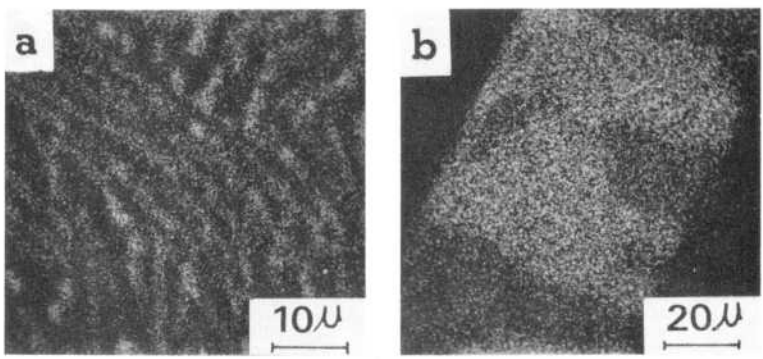

FIG. 5. (a) Cu x-ray distribution map in $Ag_{48}Zn_{50}Cu_2$ (230°C for 25 hr). (b) Au x-ray distribution map in $Ag_{48}Zn_{50}Au_2$ (275°C for 744 hr).

TABLE 2
Interplanar Crystalline Distances (in angstroms) Corresponding to the ζ_0 Complex Hexagonal and β' Ordered Cubic Phases of $Ag_{48}Zn_{50}Cu_2$, $Ag_{48}Zn_{50}Au_2$, and $Ag_{50}Zn_{50}$ After the Heat Treatment and Quench Schedule Given in the Text.

hk.l	*hkl*	$Ag_{48}Zn_{50}Cu_2$	$Ag_{48}Zn_{50}Au_2$		$Ag_{50}Zn_{50}$
11.0		3.78	3.73		3.74
	100			3.11	
21.0		2.46	2.46		2.47
	110			2.25	
11.1		2.25	2.23		2.26
30.0		2.18	2.22		2.19
20.1		2.13	2.12		2.13
21.1		1.85	1.86		1.85
	111			1.81	
22.1	200	1.57	1.57	1.57	1.57
00.2	210	1.40	1.40	1.40	1.40
32.1		1.33	1.33		1.33
41.1	211	1.28	1.29	1.29	1.28
33.0			1.27		
42.0		1.25	1.24		1.25
21.2		1.23			1.22
30.2		1.18	1.18		1.18
31.2	220		1.12	1.12	
51.1	300	1.10	1.05	1.05	1.10
52.1		0.99	1.00	1.00	0.99
	311			0.95	
53.0		0.94	0.94		0.95
42.2		0.93	0.93		0.94
51.2	222	0.91		0.91	0.91
53.1		0.90	0.90		0.90
62.1	320	0.87	0.87	0.87	0.87
54.0					0.85
22.3		0.84	0.84		0.84
63.0		0.83			0.83
61.1		0.82	0.82		0.82
72.0		0.81	0.81		0.81
63.1		0.80	0.80		0.80
80.1	400	0.79	0.79		0.79

Data obtained from electron microprobe analysis for the β' and ζ_0 phases gave the compositions displayed in Table 3. These data were obtained from over 30 measurements from samples given the heat and quench schedule. Results were corrected using the COR 2 computer program [13].

TABLE 3
Composition of the β′ and ζ_0 Phases After Heat Treatment and Quench

Alloy	β′	ζ_0
$Ag_{48}Zn_{50}Cu_2$	$Ag_{44}Zn_{51}Cu_5$	$Ag_{48}Zn_{50}Cu_2$
$Ag_{48}Zn_{50}Au_2$	$Ag_{47.5}Zn_{50}Au_{2.5}$	$Ag_{49.5}Zn_{50}Au_{0.5}$

ORDERING ENERGIES

The ordering energies of the nearest neighbors of Au–Zn and Ag–Cu pairs were calculated using the following equation, valid for ternary β-brass type alloys of nearly stoichiometric composition (coordination number $Z = 8$, $C_A \cong C_B \cong 0.5$, and $\omega_{A_gZ_n}/kT_0 \cong 0.575$ using the quasi-chemical approximation) [14]:

$$\frac{T_0' - T_0}{T_0} \cong 49\left\{1 - \frac{49}{48}\left[1 \Big/ \cosh^2\left(\frac{\omega_{AC} - \omega_{BC}}{kT}\right)\right]\right\} C_C,$$

where

T_0 is the binary base alloy order–disorder temperature ($T_0 = 233$°C for $Ag_{50}Zn_{50}$ [3]);
T_0' is the ternary alloy order–disorder temperature ($T_0' = 256$°C for $Ag_{48}Zn_{50}Cu_2$ and 296°C for $Ag_{48}Zn_{50}Au_2$ from results in this paper);
k is the Boltzman constant;
C_C is the concentration of the C atoms in the ternary alloy ($C_C = 0.02$ in this case);
ω_{AC} is the ordering energy of the A–C pair ($\omega_{CuZn} = 0.0375$ eV, obtained by extrapolating from $Cu_{50}Zn_{50}$ values [15], and $\omega_{AgAu} = 0.016$ eV, obtained from x-ray investigation [16]); and ω_{BC} is the ordering energy of the B–C pair (ω_{AgCu} or ω_{AuZn}).

The ordering energies of the nearest neighbors of the Au–Zn and Ag–Cu pairs were found to be

$$\omega_{Au-Zn} = +0.086 \text{ eV} \quad (+0.070 \text{ eV}),$$

$$\omega_{Ag-Cu} = -0.015 \text{ eV} \quad (-0.0124 \text{ eV}).$$

The values in parentheses are those obtained by Murakami et al. [17] and are in both cases slightly lower than those obtained in the present investigation.

Discussion

The order–disorder temperature T_0 measured in $Ag_{48}Zn_{50}Au_2$ fits fairly well to the extrapolated T_0 vs composition curve of Brooks and Smith [8]. T_0 measured in $Ag_{48}Zn_{50}Cu_2$ is slightly greater than that determined by Yono et al. [9] in the alloy $Ag_{51}Zn_{47}Cu_2$ (T_0 = 248°C). This discrepancy may be due to the difference in the binary base alloy composition.

The optical metallography, electron microanalysis, and x-ray results show a two-phase field ($\zeta_0 + \beta'$) in the $Ag_{48}Zn_{50}Au_2$ alloy between 250 and 275°C, the working temperature range. This two-phase field could extend at most up to the ordering temperature (296°C). The lower limit could be considered very close to 250°C, taking into consideration the length of time necessary to obtain a small transformed fraction at this temperature.

After analyzing the curves plotted in Fig. 3, the possibility of a two-phase field ($\zeta_0 + \beta'$) in $Ag_{48}Zn_{50}Cu_2$ was deduced, at least in the working temperature range of 170–232°C. This was corroborated by metallographic and electron microprobe analysis. This two-phase field could extend at most up to the ordering temperature (256°C), but it is not possible to estimate the lower limit without thermodynamic measurements to permit free energy calculation.

Grateful thanks are extended to D. Hermida and T. Palacios for their help in x-ray and microprobe analysis. Financial support by the Programa Multinacional de Metalurgia sponsored by the Organization of American States is gratefully acknowledged.

References

1. M. Hansen, *Constitution of Binary Alloys*, McGraw-Hill, New York (1958), p. 63.
2. J. Kittl and A. Cabo, The $\beta' \rightarrow \zeta_0$ transformation in the AgZn system, in *The Mechanics of Phase Transformation in Crystalline Solids*, Institute of Metals (1969), pp. 260–265.
3. D. Arias and J. Kittl, AgZn system $\beta \rightarrow \beta'$ order–disorder phase transition, *Scripta Met.*, 12:1115–1120 (1978).
4. D. Arias and J. Kittl, AgZn system $\beta' \rightarrow \zeta_0$ and $\beta \rightarrow \zeta_0$ phase transformation, *Metallography* 11:429–439 (1978).
5. J. Abriata, Termodinámica de las fases β, β' y ζ_0 en el sistema Ag–Zn, Ph.D. thesis, Universidad Nacional de Cuyo, Argentina (1970).
6. H. McI. Clark, E. A. Merriman, and C. M. Wayman, Some characteristics of the $\beta \rightarrow \zeta_0$ and $\beta' \rightarrow \zeta_0$ transformation in equiatomic AgZn, *Acta Met.* 17:719–734 (1969).
7. L. Muldawer, X-ray measurement of long-range order in β-AgZn, *Appl. Phys.* 22:663–665 (1951).

8. M. E. Brookes and R. W. Smith, Long range ordering in the system AgAuZn, *Scripta Met.* 3:667–670 (1969).
9. M. Yono, H. Asano, N. Nakanishi, and S. Kachi, Zeta-phase stability in Hume–Rothery type Cu–Ag–Zn ternary alloys, *Trans. Jpn. Inst. Met.* 8:277–278 (1967).
10. R. Kikuchi and H. Sato, Characteristics of superlattice formation in fcc alloys, *Acta Met.* 22:1099–1112 (1974).
11. W. A. Johnson and E. F. Mehl, *Trans. AIME* 135:416 (1939); J. Avrami, *Chem. Phys.* 7:1103 (1939); 8:217 (1940); 9:177 (1941) [cited by J. W. Christian, *The Theory of Transformations in Metals and Alloys*, Pergamon, Elmsford, N.Y. (1965), pp. 16–22].
12. A. W. Hull and W. P. Davey, *Phys. Rev.* 17:549 (1921) [cited by B. E. Warren, *X-Ray Diffraction*, Addison-Wesley, Reading, Mass. (1969), pp. 62–67].
13. J. Hénoc, K. F. J. Heinrich, and E. L. Myklebust, A rigorous correction for quantitative electron probe microanalysis (COR 2), NBS Tech. Note 769 (1973).
14. M. A. Krivoglaz and A. A. Smirnov, *The Theory of Order–Disorder in Alloys*, MacDonald, London (1965), Ch. 20, pp. 201–223.
15. R. H. Fowler and E. A. Guggenheim, *Statistical Thermodynamics*, 4th ed., Cambridge University Press, Cambridge, England (1956), p. 589.
16. N. Norman and B. E. Warren, *J. Appl. Phys.* 22:483 (1951) (cited by Krivoglaz and Smirnov [14, p. 222]).
17. Y. Murakami, S. Kachi, N. Nakanishi, and H. Takehara, Superlattice formation in the ternary β phase alloys, *Acta Met.* 19:93–105 (1971).

Received July 1980; accepted January 1982